estimated minimum charge seems unrealistically high. Covalent interactions to various extents—especially between the polyvalent acceptor ions and SCN^-—are most probably of some importance in determining the magnitude of ΔA. A more quantitative treatment, including a mapping of Coulomb and non-Coulomb effects, must wait, however, until further systems in mixed KSCN–KF melts have been investigated.

An instructive comparison with aqueous solution data can be made. For the four systems investigated in KSCN–KF melts by us, there are reliable data on the stability of the first complexes of Co^{2+}, Cr^{3+}, VO^{2+}, and UO_2^{2+} with SCN^- and F^- as well as the second complexes of Cr^{3+} and UO_2^{2+} in water at 298 K and $I = 1.0$ or 0.5 M.[4] Hence, the standard free energy change $\Delta G_{aq}{}^{\circ\prime}{}_{298}$ for

$$(1/j)M(NCS)_j{}^{q+}(aq) + F^-(aq) \rightarrow (1/j)MF_j{}^{q+}(aq) + SCN^-(aq) \quad (9)$$

can be calculated and directly compared with $\Delta G_{melt}{}^{\circ\prime}{}_{458}$ for

$$(1/j)M(NCS)_Z{}^{p-} + F^- \rightarrow (1/j)MF_j(NCS)_{Z-j}{}^{p-} + SCN^- \quad (10)$$

in KSCN–KF melts at 458 K for $j = 1$ and 2. The quantities so obtained all refer to the exchange of *one* SCN^- for F^-. Figure 5 shows the surprisingly good correlation between $\Delta G_{melt}{}^{\circ\prime}{}_{458}$ and $\Delta G_{aq}{}^{\circ\prime}{}_{298}$. The best fitting straight line

$$\Delta G_{melt}{}^{\circ\prime}{}_{458} = k_1 \Delta G_{aq}{}^{\circ\prime}{}_{298} + k_2 \quad (11)$$

is obtained with the parameter $k_1 = 1.00 \pm 0.05$ and $k_2 = -28.9 \pm 0.8$ kJ·(mol F)$^{-1}$. The value of k_1 is of course fortuitous, but the result is nevertheless remarkable. The ligand-exchange reaction (1) obviously occurs with a gain in free energy that is 29 kJ·(mol F)$^{-1}$ larger in the molten-salt systems at 458 K *irrespective* of central ion and actual step of complexation. The underlying reason for this is of course unclear at the present stage, although it seems that the difference in free energy of transfer of the complex ions between water and molten salt largely depends on the structure of the outer coordination shell only.

Acknowledgment. A grant from the Swedish Natural Science Research Council is gratefully acknowledged.

Registry No. $UO_2(NCS)_5{}^{3-}$, 45211-62-9; $VO(NCS)_5{}^{2-}$, 21136-26-5; KSCN, 333-20-0; KF, 7789-23-3; F_2, 7782-41-4.

Supplementary Material Available: A listing of experimental emf data (6 pages). Ordering information is given on any current masthead page.

Contribution from the Instituto de Química Inorgânica Elhúyar,
CSIC, Serrano 113, E-28006 Madrid, Spain

Diantimony Tetraoxides Revisited

J. Amador, E. Gutiérrez Puebla,[†] M. A. Monge,[†] I. Rasines,* and C. Ruíz Valero[†]

Received July 16, 1987

Untwinned crystals of α- and β-Sb_2O_4 have been grown for the first time, and both crystal structures are established from X-ray single-crystal diffraction data. α-Sb_2O_4 is orthorhombic, with $a = 5.434$ (1) Å, $b = 4.8091$ (6) Å, $c = 11.779$ (2) Å, $Z = 4$, and space group $Pna2_1$ (No. 33), and β-Sb_2O_4 is monoclinic, with $a = 12.057$ (1) Å, $b = 4.8352$ (3) Å, $c = 5.384$ (2) Å, $\beta = 104.56$ (1)°, $Z = 4$, and space group $C2/c$ (No. 15). Bond distances and angles are given. In α-Sb_2O_4, Sb^VO_6 octahedra share vertices forming layers, parallel to the a–b plane, joined by pairs of $Sb^{III}O_4E$ tetragonal pyramids, which share two oxygen atoms. The Sb^VO_6 octahedra of the β form are more regular and form layers parallel to b–c, with rows of $Sb^{III}O_4E$ pairs along the c direction. In the layers of both forms one interstice exists for every four Sb^VO_6 octahedra. These interstices have to be viewed through a certain direction in β-Sb_2O_4 to appear identical with those of the α form. For both structures the packing of oxygen atoms is more dense than for cubic or orthorhombic Sb_2O_3. According to bond-valence considerations, ψ-tetragonal-pyramidal coordination of Sb(III) can be considered as octahedral.

The first chemical analysis of Sb_2O_4 was performed in 1845 by Dufrênoy[1] on a sample from Cervantes (Lugo, Spain). Five years later Dana designated this mineral as cervantite.[2] For lack of suitable crystals, in 1938 Dihlström[3] had to infer the structure of synthetic cervantite from that of isomorphous stibiotantalite, $SbTaO_4$, which is orthorhombic, space group $Pna2_1$ (No. 33), $Z = 4$. In 1960 the unit cell dimensions of synthetic cervantite were determined,[4] and 2 years later it was established that the mineral shows the same X-ray diffraction pattern as synthetic cervantite. From crystals obtained by oxidation in air of Sb_2O_3, in 1975 the crystal structure of Sb_2O_4 was refined[5] in space group $Pna2_1$, obtaining an R factor of 0.107. More recently[6] the structure of synthetic Sb_2O_4 has been determined by a profile analysis of powder neutron diffraction data. The refinement in space group $Pna2_1$ converged to $R = 0.0685$ by using isotropic temperature factors, which were negative for Sb atoms.

In 1964, a new form of Sb_2O_4, designated as β-Sb_2O_4, was described.[7] The crystals were monoclinic prisms, elongated along c, with (100) prominent and were polysynthetically twinned on (100) with b and c in common. The structure was refined in space group $C2/c$ (No. 15), $Z = 4$, by using isotropic temperature factors, to $R = 0.066$.

In the course of our studies of Sb oxides, we have repeatedly attempted growing α- and β-Sb_2O_4 crystals under different conditions. At last, we obtained for the first time one crystal of α-Sb_2O_4 and, simultaneously, some nontwinned crystals of β-Sb_2O_4. The work reported here describes both crystal structures, making a comparison between them.

Table I. Coefficients for the Weighting Scheme in α-Sb_2O_4

	a	*b*		*c*	*d*
$\lvert F_o \rvert < 36$	7.55	−0.17	$(\sin\theta)/\lambda < 0.51$ Å^{-1}	2.24	−3.37
$36 < \lvert F_o \rvert < 310$	1.09	0.02	$0.51 < (\sin\theta)/\lambda < 0.71$	−2.11	5.08

Experimental Section

Crystal Growth. Crystals were grown by heating polycrystalline analytical grade α-Sb_2O_4 in evacuated (10^{-3} mmHg) quartz ampules, after three successive treatments at 963, 1073, and 1223 K, each one

---

[†] Present address: Departamento de Química Inorgânica, Facultad de Ciencias Químicas, Universidad Complutense, E-28006 Madrid, Spain.

(1) Dufrênoy, A. *Traité de Minéralogie*; Carilian Goevry et Vr. Dalmont Editeurs: Paris, 1845; Vol. 2. pp 654-5.

(2) Gründer, W.; Pätzold, H.; Strunz, H. *Neues Jahrb. Mineral., Monatsh.* **1962**, *5*, 93.

(3) Dihlström, K. *Z. Anorg. Allg. Chem.* **1938**, *239*, 57.

(4) Swanson, H. E.; Cook, M. I.; Evans, E. H.; de Groot, S. H. *Natl. Bur. Stand. Circ. (U.S.)* **1960**, *539*, 8.

(5) Gopalakrishnan, P. S.; Manohar, H. *Cryst. Struct. Commun.* **1975**, *4*, 203.

(6) Thornton, G. *Acta Crystallogr. Sect. B: Struct. Crystallogr. Cryst. Chem.* **1977**, *B33*, 1271.

(7) Rogers, D.; Skapski, A. C. *Proc. Chem. Soc.* **1964**, 400.

0020-1669/88/1327-1367$01.50/0

Table II. Atomic Coordinates for α-Sb_2O_4 and β-Sb_2O_4 with Estimated Standard Deviations (Esd's) in Parentheses

	x/a	y/b	z/c
		α-Sb_2O_4	
Sb1	0.3727 (2)	−0.0008 (4)	0.2483 (4)
Sb2	−0.0225 (3)	0.0358 (2)	0.0000 (0)
O1	0.3175 (36)	0.1572 (47)	0.0952 (19)
O2	0.1512 (31)	0.7054 (37)	0.1912 (15)
O3	0.0822 (32)	0.2021 (37)	0.3052 (15)
O4	0.3518 (30)	0.8320 (38)	0.4076 (16)
		β-Sb_2O_4	
Sb1	0.2500 (0)	0.2500 (0)	0.0000 (0)
Sb2	0.0000 (0)	0.2865 (2)	0.2500 (0)
O1	0.1908 (8)	0.0516 (19)	0.6749 (17)
O2	0.0946 (8)	0.4132 (20)	0.9637 (17)

lasting 24 h, followed by quenching in liquid nitrogen.

Crystallographic Study. Clear, colorless, prismatic crystals of sizes 0.04 × 0.04 × 0.06 (α) and 0.04 × 0.02 × 0.05 mm^3 (β), respectively, were mounted in a Nonius CAD-4 diffractometer. The cell dimensions were refined by least-squares fitting of the 2θ values of 25 reflections. Intensities of 498 reflections within $1° < \theta < 30°$ and indexes from (0,0,0) to (7,6,16) for α and 442 reflections within $1° < \theta < 25°$ from (−16,0,0) to (16,6,7) for β were measured at 295 K with monochromatic Mo Kα radiation (λ = 0.71069 Å) and an $\omega/2\theta$ scan technique. There was no appreciable drop in intensity of standard reflections, three for α and two for β, checked every hour in both cases. R_i was 0.0302 and 0.0169 for the α and β forms, respectively. Intensities were corrected for Lorentz and polarization effects, and 377 and 414 ($I > 2\sigma(I)$) were considered as observed for the α and β oxides, respectively. Scattering factors for neutral atoms and anomalous dispersion corrections for Sb were taken from ref. 8. Both structures were solved by Patterson and Fourier syntheses. Empirical absorption corrections[9] were applied at the end of the isotropic refinements. The maximum and minimum absorption factors were 1.265 and 0.854, respectively, for α-Sb_2O_4, and 1.304 and 0.864, respectively, for the β form. In the case of α-Sb_2O_4, the z coordinate of Sb2 was fixed, and mixed full-matrix least-squares (LS) refinement with anisotropic temperature factors for the Sb atoms, isotropic temperature factors for oxygen, and unit weights minimizing the function $\sum w(|F_o| - |F_c|)^2$ led to R = 0.039. In order to prevent bias on $\langle F \rangle$ vs $\langle F_o \rangle$ or $\langle(\sin\theta)/\lambda\rangle$, the last steps of the refinement were calculated by PESOS[10] with weights $w = w_1 w_2$, where $w_1 = 1/(a + b|F_o|)^2$ and $w_2 = 1/(c + d(\sin\theta)/\lambda)$, and the coefficients shown in Table I. The final R was 0.039 and $R_w = (\sum w\Delta^2/\sum w|F_o|^2)^{1/2}$ = 0.046. Maximum and average shift-to-error ratios in the final LS cycle were 0.26 and 0.06, respectively. For β-Sb_2O_4 anisotropic full-matrix least-squares refinement with unit weights led to R = 0.042 and R_w = 0.052. No trend in F vs F_o or $(\sin\theta)/\lambda$ was observed. Maximum and average shift-to-error ratios were 0.05 and 0.001. Most of the calculations were carried out with X-RAY 80.[11]

Results

Crystal Growth. After the thermal treatments indicated, crystals appeared on the yellowish white surface of a melt of polycrystalline α-Sb_2O_4, which remained at the lower part of the ampules.

Crystal Data. α-Sb_2O_4, M_r = 307.50, is orthorhombic, with a = 5.434 (1) Å, b = 4.8091 (6) Å, c = 11.779 (2) Å, V = 307.82 (9) Å^3, Z = 4, D_{calcd} = 6.63 g cm^{-3}, $F(000)$ = 536, μ(MoKα) = 175.06 cm^{-1}, space group $Pna2_1$ (No. 33), R = 0.039, and R_w = 0.046 for 377 observed reflections.

β-Sb_2O_4, M_r = 307.50, is monoclinic, with a = 12.057 (1) Å, b = 4.8352 (3) Å, c = 5.384 (2) Å, β = 104.56 (1)°, V = 303.8 (2) Å^3, Z = 4, D_{calcd} = 6.72 g cm^{-3}, $F(000)$ = 536, μ(Mo Kα) = 177.38 cm^{-1}, space group $C2/c$ (No. 15), R = 0.042, and R_w = 0.052 for 414 observed reflections.

Atomic coordinates for α- and β-Sb_2O_4 are shown in Table II. Table III includes bond lengths and angles.

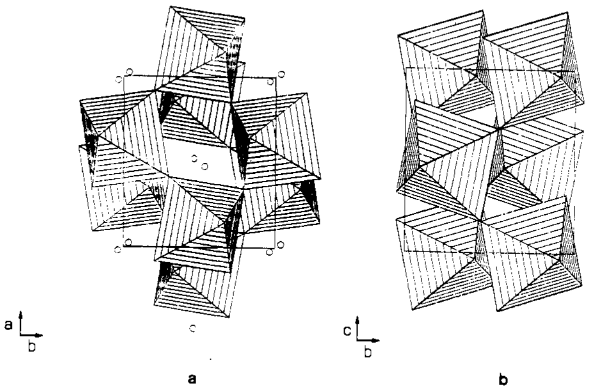

Figure 1. STRUPLO[14] view of the unit cell of (a) α-Sb_2O_4 (*ab*) and (b) β-Sb_2O_4 (*bc*).

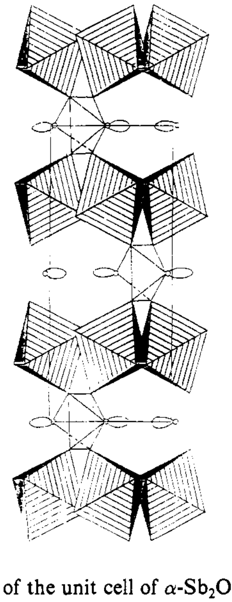

Figure 2. STRUPLO[14] view of the unit cell of α-Sb_2O_4 (*ac*), showing the lone pair of Sb2 and the coordination of Sb2 to the four nearest oxygen atoms.

Description of the Structures. Two kinds of Sb atoms have to be distinguished in the α form. Those of pentavalent Sb1 are coordinated to six oxygens situated at the vertices of a slightly distorted octahedron. If the magnitude of distortion is defined by $\delta = 10^4\sum[(r_i - r_m)/r_m]^2$, then for the Sb^VO_6 octahedra, δ = 24. On the other hand, trivalent Sb2, with one electron lone pair, E, is coordinated to four oxygen atoms situated at 2.0–2.2 Å. Although these atoms are not coplanar, the coordination polyhedron $Sb^{III}O_4E$ can be conceived as a tetragonal pyramid containing Sb2 at the center, four basal oxygen atoms, and the apical vertex at which the nonbonded electron pair is pointing. Sb^VO_6 octahedra are joined by sharing vertices and forming layers, in which one interstice exists for every four octahedra, as shown in Figure 1a, and every two $Sb^{III}O_4E$ pyramids have in common two oxygen atoms. As Figure 2 shows, the α crystal is formed by layers of Sb^VO_6 octahedra that are parallel to the *ab* plane and are joined by pairs of Sb(III) atoms. These atoms form rows parallel to the Sb^VO_6 octahedra layers and share two oxygen atoms, as has been noted. Two oxygen atoms of the $Sb^{III}O_4E$ pyramids are situated in the upper layer, and the other two lie in the lower.

Although β-Sb_2O_4 is monoclinic, $C2/c$, and the α form is orthorhombic, $Pna2_1$, both structures are similar, as suggested at first sight by the resemblance of the lattice parameters, if a and c are interchanged. In β form Sb(III) are situated on twofold axes, and Sb(V) atoms occupy symmetry centres, making Sb^VO_6 octahedra more regular (δ = 3); the layers of Sb^VO_6 octahedra are parallel to *bc*, being the rows of Sb(III) pairs lying along the c direction. Figure 1b shows the interstices formed by four octahedra of the same layer in the β form. These interstices are similar to those of α-Sb_2O_4 (Figure 1a), although they cannot be

---

(8) *International Tables for X-Ray Crystallography*; Kynoch: Birmingham, U.K., 1974; Vol. IV, p 72.

(9) Walker, N.; Stuart, S. *Acta Crystallogr., Sect. A: Found. Crystallogr.* **1983**, *A39*, 158.

(10) Martinez Ripoll, M.; Cano, F. H. "PESOS Program"; Instituto Rocasolano, CSIC: Madrid, Spain, 1975.

(11) Stewart, J. M.; Kundell, F. A.; Baldwin, J. C. "The X-Ray 80 System"; Computer Science Center, University of Maryland: College Park, Maryland, 1980.

Table III. Interatomic Distances (Å) and Angles (deg) in α-Sb_2O_4 and β-Sb_2O_4[a]

	esd's dist	esd's angles
α-Sb_2O_4	0.019	0.7
β-Sb_2O_4	0.009	0.4

α-Sb_2O_4		β-Sb_2O_4	
Sb1–O1	1.980	Sb1–O1^{1}	1.966
Sb1–O2^{8}	1.974	Sb1–O1^{2}	1.966
Sb1–O2^{9}	1.927	Sb1–O1^{3}	1.965
Sb1–O3	1.973	Sb1–O1^{4}	1.965
Sb1–O3^{9}	1.951	Sb1–O2^{1}	1.997
Sb1–O4^{8}	2.044	Sb1–O2^{2}	1.997
Sb2–O1	2.238	Sb2–O1^{4}	2.932
Sb2–O1^{10}	2.048	Sb2–O1^{13}	2.932
Sb2–O2^{8}	2.913	Sb2–O2^{1}	2.221
Sb2–O3^{14}	2.584	Sb2–O2^{5}	2.018
Sb2–O4^{11}	2.189	Sb2–O2^{6}	2.221
Sb2–O4^{12}	2.019	Sb2–O2^{7}	2.018
O1–Sb1–O2^{8}	82.6	O1–Sb1–O1^{2}	180.4
O1–Sb1–O2^{9}	89.8	O1–Sb1–O1^{3}	91.7
O1–Sb1–O3	89.9	O1–Sb1–O1^{4}	88.3
O1–Sb1–O3^{9}	96.8	O1–Sb1–O2^{1}	89.1
O1–Sb1–O4^{8}	168.1	O1–Sb1–O2^{2}	90.9
O2^{8}–Sb1–O2^{9}	89.7	O1^{3}–Sb1–O2^{1}	96.0
O2^{8}–Sb1–O3	89.0	O1^{3}–Sb1–O2^{2}	84.0
O2^{8}–Sb1–O3^{9}	178.1	O1^{4}–Sb1–O2^{2}	180.0
O2^{8}–Sb1–O4^{8}	89.8	O1^{4}–Sb2–O1^{13}	112.2
O2^{9}–Sb1–O3	178.6	O1^{4}–Sb2–O2^{1}	60.1
O2^{9}–Sb1–O3^{9}	92.2	O1^{4}–Sb2–O2^{5}	132.3
O2^{9}–Sb1–O4^{8}	99.4	O1^{4}–Sb2–O2^{6}	143.8
O3–Sb1–O3^{9}	89.2	O1^{4}–Sb2–O2^{7}	97.4
O3–Sb1–O4^{8}	80.7	O1^{13}–Sb2–O2^{1}	143.8
O3^{9}–Sb1–O4^{8}	90.4	O2^{1}–Sb2–O2^{7}	132.3
O1–Sb2–O1^{10}	93.6	O2^{1}–Sb2–O2^{5}	73.0
O1–Sb2–O2^{8}	59.2	O2^{1}–Sb2–O2^{6}	148.0
O1–Sb2–O3^{14}	131.6	O2^{1}–Sb2–O2^{7}	83.2
O1–Sb2–O4^{11}	148.0	O2^{5}–Sb2–O2^{7}	88.0
O1–Sb2–O4^{12}	73.0	O2^{6}–Sb2–O2^{7}	73.8
O1^{10}–Sb2–O2^{8}	96.2		
O1^{10}–Sb2–O4^{11}	73.5		
O1^{10}–Sb2–O4^{12}	88.9		
O2^{8}–Sb2–O3^{14}	119.0		
O2^{8}–Sb2–O4^{11}	143.9		
O2^{8}–Sb2–O4^{12}	130.8		
O3^{14}–Sb2–O4^{12}	83.8		
O4^{11}–Sb2–O4^{12}	84.4		
O4^{11}–Sb2–O3^{14}	65.4		
O3^{14}–Sb2–O1^{10}	138.7		

[a] Symmetry transformations: (1) $x, y, z-1$; (2) $^1/_2-x, {}^1/_2-y, 1-z$; (3) $^1/_2-x, {}^1/_2+y, {}^1/_2-z$; (4) $x, -y, z-{}^1/_2$; (5) $-x, 1-y, 1-z$; (6) $-x, y, {}^3/_2-z$; (7) $x, 1-y, z-{}^1/_2$; (8) $x, y-1, z$; (9) $^1/_2+x, {}^1/_2-y, z$; (10) $x-{}^1/_2, {}^1/_2-y, z$; (11) $-x, 1-y, z-{}^1/_2$; (12) $^1/_2-x, y-{}^1/_2, z-{}^1/_2$; (13) $-x, -y, 1-z$; (14) $-x, -y, z-{}^1/_2$.

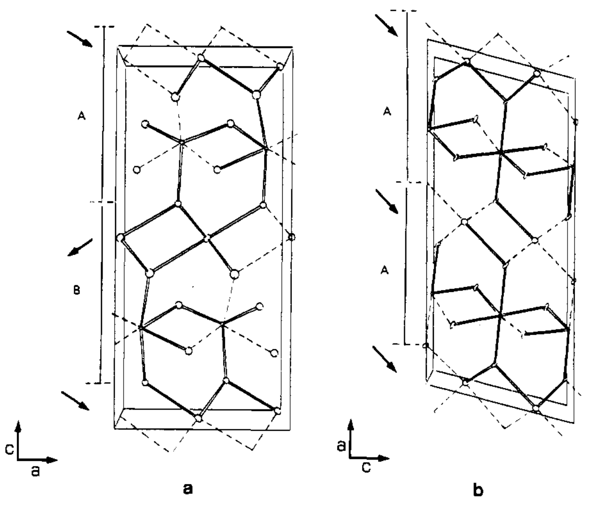

Figure 3. ORTEP[15] perspective of the (a) α-Sb_2O_4 and (b) β-Sb_2O_4 unit cells viewed in the *b* direction. Broken lines show interatomic distances to adjacent cells.

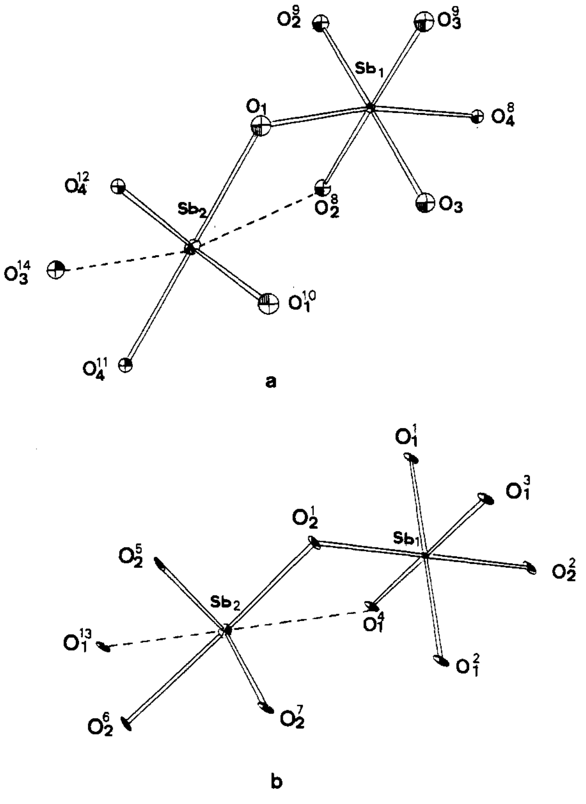

Figure 4. Coordination polyhedra of Sb atoms in (a) α-Sb_2O_4 and (b) β-Sb_2O_4.

visualized in the same way because the angle β is not 90°. When the interstices shown in Figure 1b are viewed through a certain direction imposed by that angle, they look identical with those of Figure 1a.

A perspective of the α and β unit cells in the *b* direction is shown in Figure 3. Besides the displacement of the origin, the main difference between both cells is related to the disposition of the slices formed by one layer of $Sb^{V}O_6$ octahedra and one row of double $Sb^{III}O_4E$ pyramids. As a consequence of the existence of an *n* plane, perpendicular to *a*, these slices alternate, ABAB..., as shown in Figure 3. In the β form they repeat, AA..., as in the same figure.

Discussion

The unit cell parameters for α-Sb_2O_4 now measured agree fairly well with those established by Swanson et al.,[4] a = 5.436, b = 4.810, and c = 11.76 Å. However the present crystal structure determination of the α form shows some differences with those of previous studies.[5,6] One of them[5] gives an *R* value of 0.107 and large estimated standard deviations (esd) for interatomic distances, for example 1.93 (5) and 2.00 (5) Å for Sb2–O3 and Sb2–O4, respectively. In the second study[6] large esd values for atomic positional parameters and very small values for interatomic distances were obtained; for instance, a value of z = 0.009 (1) for Sb1 and the distance Sb1–O4 = 1.172 (1) Å are observed. The esd of our interatomic distances, 0.019 Å, though larger, is consistent with the esd that we obtain for the atomic positional parameters. On the other hand, in the same study[6] negative and equal thermal factors for Sb1 and Sb2, B = –0.13 (6) Å^2, and the same thermal parameter for all oxygen atoms, B = 0.31 (5) Å^2, were obtained. Perhaps both results can be attributed to absorption and extinction effects, whose corrections were not made. In our case anisotropic factors for Sb1 and Sb2 and positive isotropic factors for the oxygen atoms have been obtained.

The cell volumes per anion for α- and β-Sb_2O_4 are 19.2 and 19.0 Å^3, respectively, whereas they equal[12] 27.6 and 28.9 Å^3 for orthorhombic and cubic Sb_2O_3. If the volume of the Sb^{III} cation together with its lone pair is computed like that of an oxygen atom, these figures lower to 15.4 and 15.2 Å^3 for Sb_2O_4 and 16.6 and 17.3 Å^3 for the two forms of Sb_2O_3. This indicates that the oxygen packing in α- and β-Sb_2O_4 is more dense than in the case of orthorhombic and cubic Sb_2O_3.

As indicated in Figure 4, the coordination of trivalent Sb2 in both forms of Sb_2O_4 can also be considered as very distorted octahedral (δ = 1613 and 1150, for α and β forms, respectively), if two more oxygen atoms at relatively larger distances are taken into account. When only the four shortest Sb2–O distances of Table III (between 2.019 and 2.238 Å for α-Sb_2O_4 and between 2.018 and 2.221 Å for the β form) are considered, the sums of the bond valences of Sb(III) equal 2.58 and 2.55, rather low values for trivalent Sb of α- and β-Sb_2O_4, respectively. However, taking into account two additional bonds (2.584 and 2.913 Å for the α form and two bonds of 2.932 Å for β-Sb_2O_4) the sums of the bond valences for both Sb(III) atoms become close to 3, 2.95 for α-Sb_2O_4 and 2.87 in the case of β-Sb_2O_4. On the other hand, the sums of the bond valences[13] for pentavalent Sb1 are 4.96 and 4.91 for the α and β forms, respectively.

Acknowledgment. We acknowledge a fellowship to C.R.V. and the financial aid of the Consejo Superior de Investigaciones Científicas.

Registry No. Sb_2O_4, 1332-81-6.

Supplementary Material Available: Listings of anisotropic thermal parameters for α-Sb_2O_4 and β-Sb_2O_4 (1 page); listings of observed and calculated structure factors for α-Sb_2O_4 and β-Sb_2O_4 (6 pages). Ordering information is given on any current masthead page.

---

(12) Gutiérrez Puebla, E.; Gutiérrez Rios, E.; Monge, A.; Rasines, I. *Acta Crystallogr., Sect. B: Struct. Crystallogr. Cryst. Chem.* **1982**, *B38*, 2021.

(13) Brown, I. D.; Wu, K. K. *Acta Crystallogr., Sect. B: Struct. Crystallogr. Cryst. Chem.* **1976**, *B32*, 1957.

(14) Fischer, R. X. *J. Appl. Crystallogr.* **1985**, *18*, 258.

(15) Johnson, C. K. "ORTEP, A Fortran thermal-ellipsoid plot program for crystal structure illustrations"; Report ORNL-3794; Oak Ridge National Laboratory: Oak Ridge, TN, 1965.

Contribution from the Department of Inorganic Chemistry, University of Umeå, S-901 87 Umeå, Sweden,
and Department of Physical Chemistry, Ruder Bošković Institute, Bijenička 54, YU-41001 Zagreb, Yugoslavia

Equilibrium and Structural Studies of Silicon(IV) and Aluminum(III) in Aqueous Solution. 16. Complexation and Precipitation Reactions in the H^+–Al^{3+}–Phthalate System

T. Hedlund,[†] H. Bilinski,[‡] L. Horvath,[‡] N. Ingri,[†] and S. Sjöberg*[†]

Received September 23, 1987

Equilibria in the title system were studied in 0.6 mol dm^{-3} Na(Cl) medium (25 °C) by using potentiometric (glass electrode) and tyndallometric methods. The Al complexation is characterized by the formation of the binary species AlL^+ and AlL_2^- as well as by the polynuclear mixed hydroxo complexes $Al_3(OH)_4L^{3+}$, $Al_2(OH)_2L^{2+}$, and $Al_2(OH)_2L_2$. The mononuclear species are of intermediate stability ($\log \beta_1 = 2.94 \pm 0.02$, $\log \beta_2 = 4.97 \pm 0.14$), whereas the polynuclear complexes show a higher stability (cf. $\log k(Al_3(OH)_4{}^{5+} + L^{2-} \rightleftarrows Al_3(OH)_4L^{3+}) = 5.10 \pm 0.03$). A solid phase with the composition $Al_2(OH)_4L\cdot 4H_2O$ was found to determine the precipitation boundary. The following formation constant was deduced: $\log k(2Al^{3+} + L^{2-} + 4H_2O \rightleftarrows Al_2(OH)_4L(s) + 4H^+) = 8.44 \pm 0.08$. This phase may be considered as the first precipitation step in the hydrolysis of aqueous aluminum phthalates to stable aluminum hydroxide and aluminate ions. The solid phase has also been characterized from X-ray analysis of powders, TGA, and IR spectra. Considering the phthalate ion as a possible binding site in humic substances, the significance of complexation and precipitation reactions in natural waters are discussed.

Introduction

The present work forms part of a research program on complexation and precipitation reactions in aluminosilicate systems comprising different organic ligands. In preceding publications homogenous[1] and heterogenous[2] equilibria characterizing the subsystem H^+–Al^{3+}–oxalic acid were studied. By the combination of results from precise equilibrium-analytical solution data with precipitation boundary data, it became possible to determine the composition and stability of the solid phases formed. It was found that the formed precipitates could be considered as the first metastable phases in the hydrolytic transformation of the aqueous AlL_n complexes down to stable aluminum hydroxide. This transition could be written as a series of complexation–hydrolysis reactions according to the scheme

$$Al^{3+} \rightleftarrows AlL_n(aq) \rightleftarrows Al_q(OH)_pL_r(aq) \rightleftarrows Al_q(OH)_pL_r(s) \rightleftarrows Al(OH)_3(s) \rightleftarrows Al(OH)_4^-$$

Out of the two phases formed, $Al_3(OH)_7Ox\cdot 3H_2O$ (Ox = oxalate) was found to be a possible solid phase in oxalate-rich (>$10^{-4.9}$ mol dm^{-3}) natural waters. Furthermore, this phase was indicated to have an octahedrally ordered sheet structure where oxalate ions were chelated on the sheet surface functioning as a bridge between two Al atoms. The ligands in this layer may then be substituted by various other ligands, e.g. silicic acid or silicate ions. Such a Si substitution may be the first step in an initial clay formation.

The objective of the present study is to study complexation and precipitation reactions in another subsystem, viz. the H^+–Al^{3+}–phthalate (L^{2-})–Na^+ system. Phthalate (L^{2-}) was chosen as a simple ligand containing carboxylic groups with an aromatic ring, both characteristic of natural humic substances. To our knowledge a complete characterization of these reactions has not been presented before. According to Napoli and Liberti,[3] the Al speciation is given by the two species AlL^+ ($\log k_1 = 3.18$) and AlL_2^- ($\log k_2 = 3.14$). The measurements were performed at 25 °C in 0.5 M $NaClO_4$ with $-\log [H^+] \leq 3.5$, where the possible formation of mixed Al^{3+}–L^{2-}–OH^- complexes was neglected. As these types of species frequently are formed, especially close to the precipitation boundaries, a full understanding of precipitation reactions and mechanisms is not possible unless such species are taken into consideration.

[†] University of Umeå.

[‡] Ruder Bošković Institute.

(1) Sjöberg, S.; Öhman, L.-O. *J. Chem. Soc., Dalton Trans.* **1985**, 2665.

(2) Bilinski, H.; Horvath, L.; Ingri, N.; Sjöberg, S. *Geochim. Cosmochim. Acta* **1985**, *50*, 1911.

(3) Napoli, A.; Liberti, A. *Gazz. Chim. Ital.* **1970**, *100*, 906.

0020-1669/88/1327-1370$01.50/0